Electronic Supplementary Material (ESI) for Physical Chemistry Chemical Physics

Electronic Supporting Information

One-photon excited luminescence of single gold particles diffusing in solution under pulsed illumination.

Matthieu Loumaigne*[a,b], Priya Vasanthakumar[c,d], Anna Lombardi[a], Alain Richard[c] and Anne Débarre*[c,e]

[a] *FemtoNanoOptics group, LASIM, Univ. Lyon 1-CNRS, 43 Boulevard du 11 Novembre, F-69622, Villeurbanne cedex, France.*
[b] *BIOMIS group, ENS Cachan - Bretagne Campus de Ker Lann Avenue Robert Schuman, F- 35170 BRUZ, France ; E-mail : matthieu.loumaigne@bretagne.ens-cachan.fr.*
[c] *Laboratoire Aimé Cotton, CNRS, Univ. Paris-Sud, Bâtiment 505, F-91405 Orsay cedex, France, tel 33 1 69 35 21 02 ; E-mail : anne.debarre@lac.u-psud.fr*
[d] *Dipartimento di Fisica "Enrico Fermi", Universita' di Pisa, Largo Bruno Pontecorvo, 3, 56127 Pisa, Italy.*
[e] *PPSM, ENS Cachan, CNRS, Univ. Paris-Sud, 61 avenue du Président Wilson, F-94235 Cachan Cedex, France, tel : 33 1 47 40 74 43; E-mail : anne.debarre@ppsm.ens-cachan.fr*

A. OPL fluorescence correlation profile of gold spherical particles of 20nm diameter.

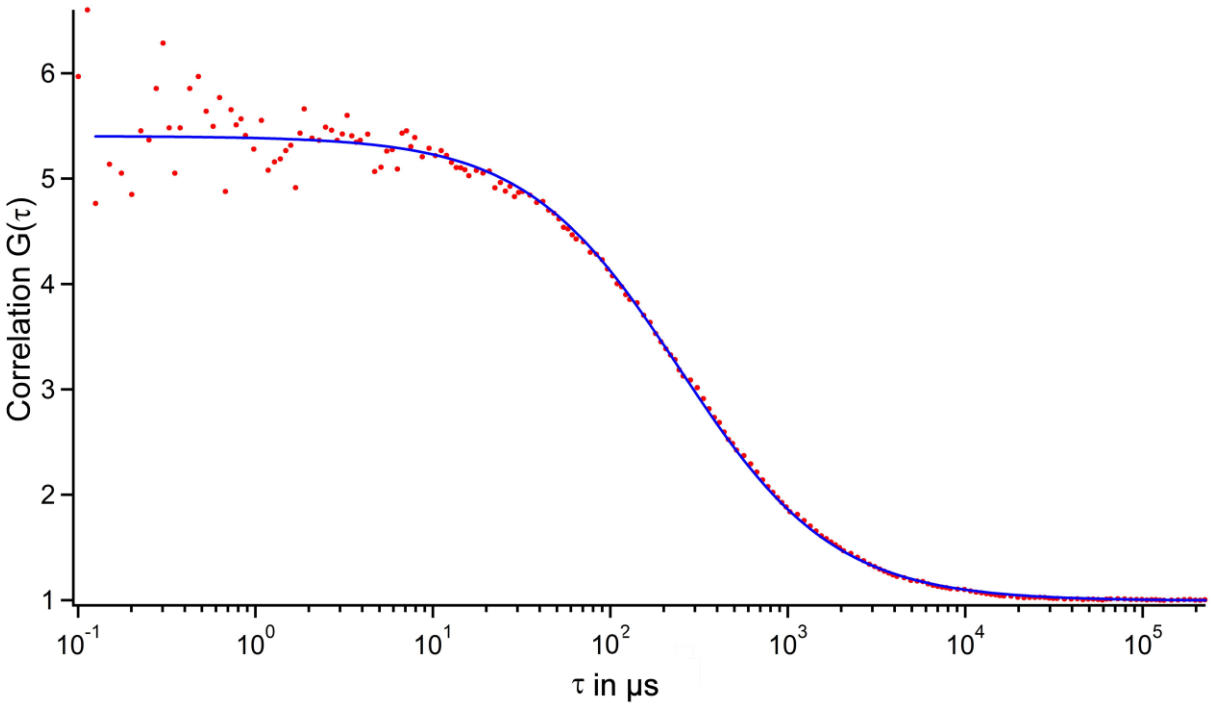

Figure S1. Correlation of OPL signal of 20nm gold spherical particles excited at 470nm with an average irradiance of 50kW/cm² and a 100fs pulsed laser.

In order to get rid of the Raman scattering contribution of the water, the signal is filtered by a band pass filter selecting 520-530nm. Contrary to the TPL signal of gold spherical particles of same diameter,[7] there is no anisotropy and there is no rotation contribution in the FCS profile. The diffusion time deduced from the fit corresponding to the model of a freely diffusing species assuming a gaussian observation volume is 260 µs. This diffusion time corresponds to a hydrodynamical diameter of 11nm. 20nm gold nanobead exhibit a decrease of the diffusion time with the laser power as it is observed for the 50 nm diameter particles.

B. Histogram of TPL at 820nm.

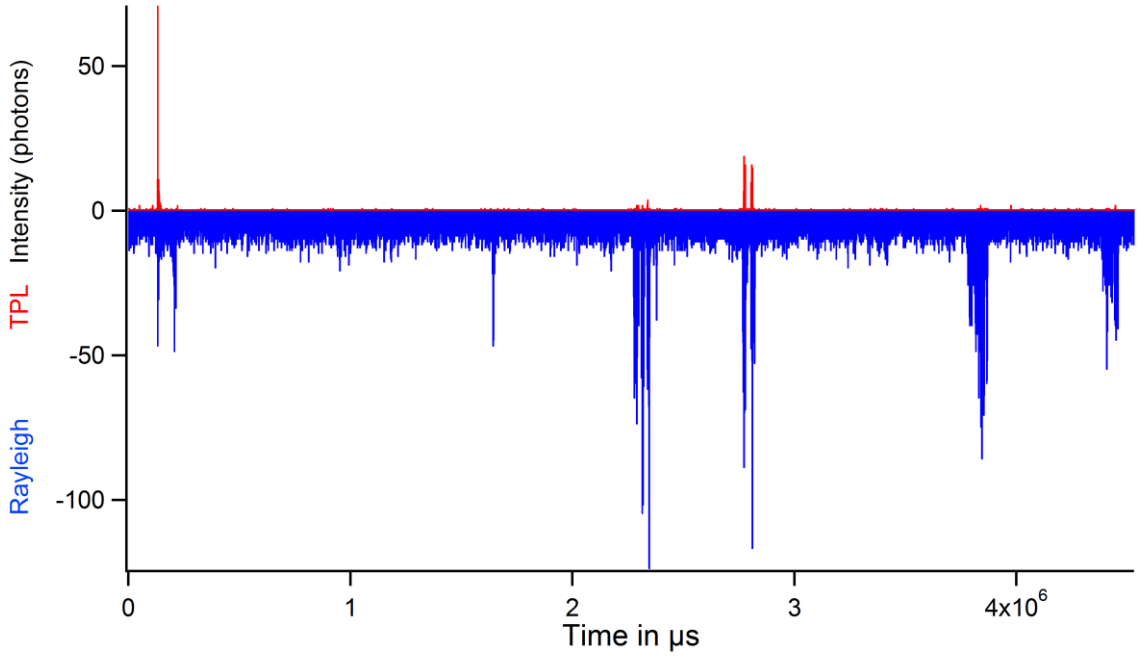

Figure S2. Dual histogram of 50 nm diameter gold particles excited at 820nm under pulsed excitation. Red histogram: TPL; blue histogram: corresponding Rayleigh scattering signal; average excitation irradiance 680kW/cm^2, pulse duration: 100fs, 1ms bin size.

Only a fraction of the spherical particles are luminescent at this laser irradiance. As the power increases, the number of luminescent particles increases to reach 100% as it is the case for OPL at low irradiances.

C. Evolution of the diffusion time for TPL of 20 nm diameter gold spherical particles

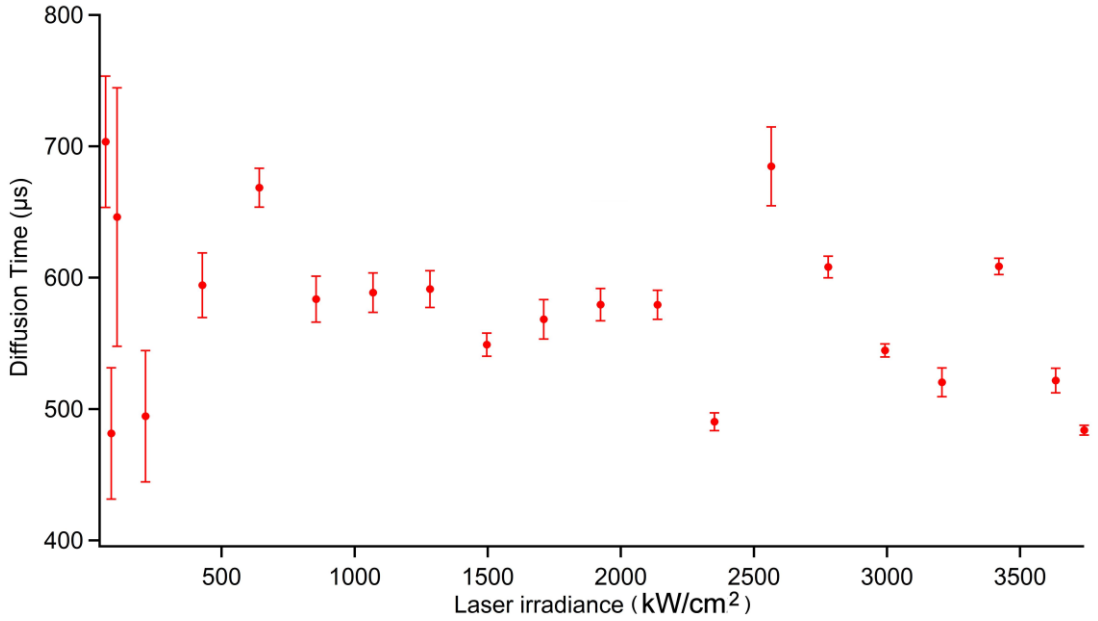

Figure S3. Diffusion times derived from FCS measurements of TPL on 20 nm diameter gold particles excited at 820nm for increasing laser irradiances.

The measurements demonstrate that the diffusion time of gold particles of 20 nm diameter does not evolve significantly with laser irradiance when TPL is excited.

D. Evolution of OPL for ensemble and single particle measurements with respect to pulsed laser irradiance.

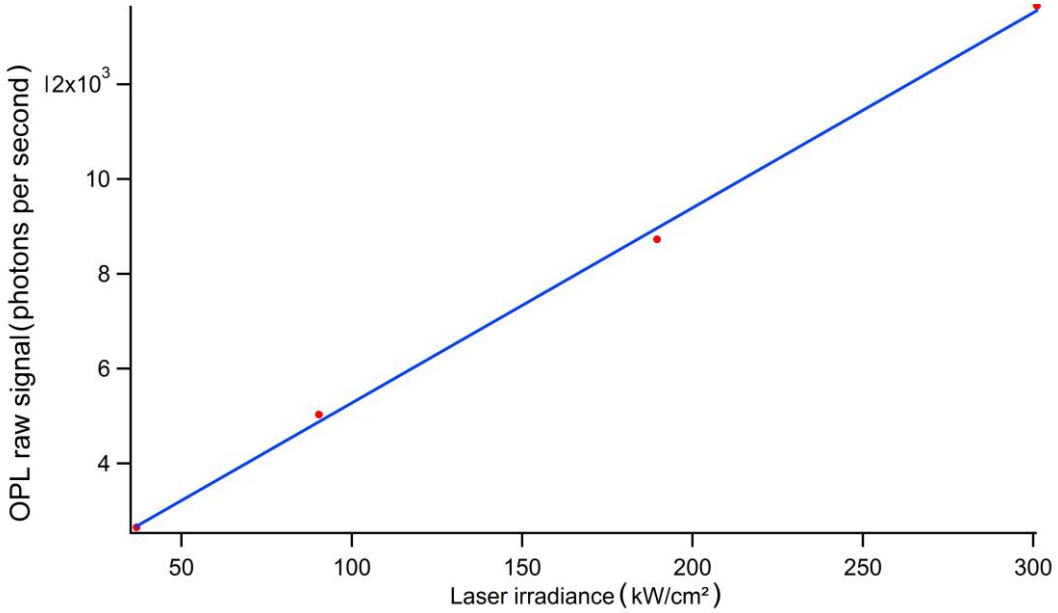

Figure S4. Ensemble OPL signal of 50 nm particles excited at 430nm with a 100fs pulsed laser for different mean laser irradiances. These data are extracted from the same measurements as those presented in Fig 4. of the main text. The signal is filtered with a long pass interferometric filter, centered at 510 nm.

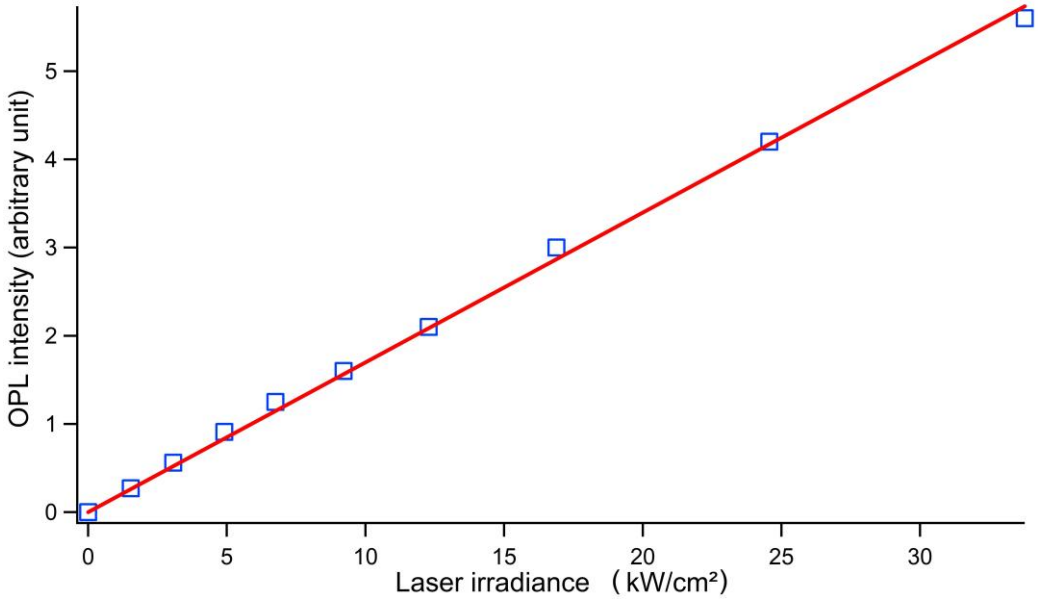

Figure S5. OPL signal of a single deposited gold spherical particle of diameter 63nm excited at 430nm with a 100fs pulsed laser for different laser irradiances.

The particle is deposited and is undergoing a spatial modulation. The laser is filtered by two long pass interferometric filters centered at 450 nm.

E. Discretization method and examples

E1 Additional examples of burst analysis

These data are extracted from the same measurements as those presented in Fig 7. of the main text, except d) wich correspond to a 50nm bead diffusing in pure water. The time step for d) is 50µs

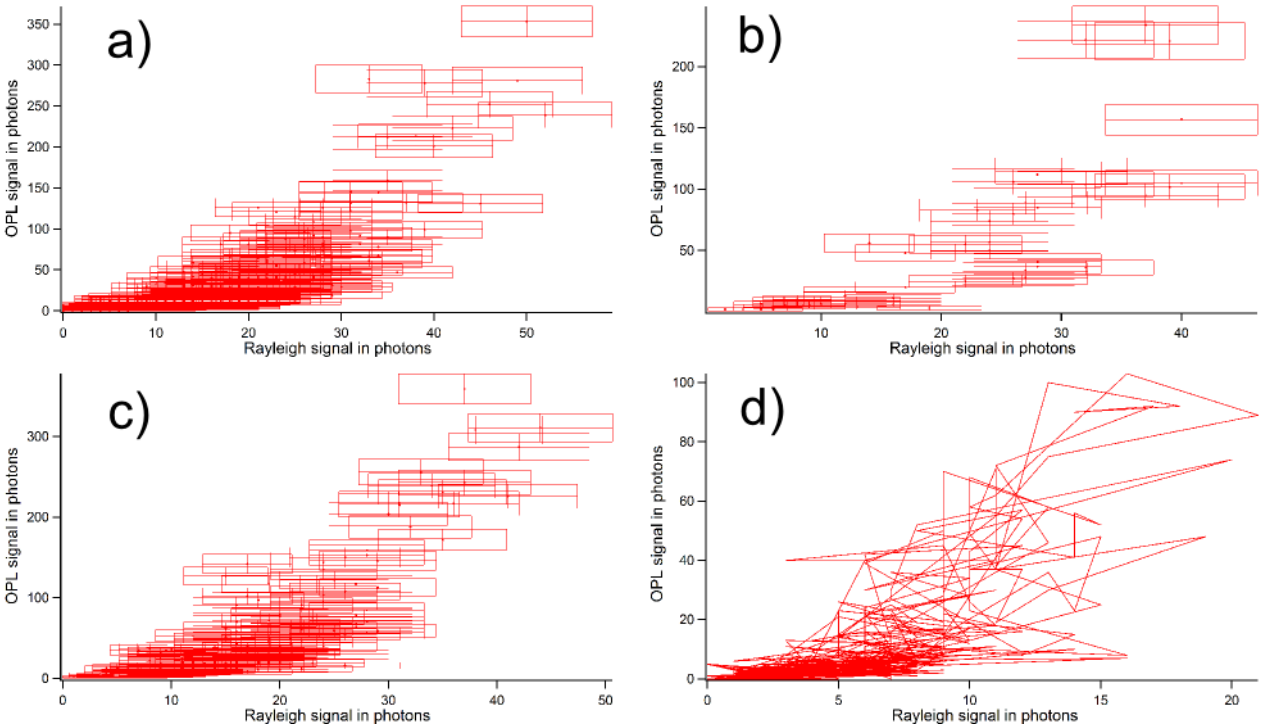

Figure S6. Intensity of luminescence with respect to light scattering intensity for a single beads of diameter 50 nm. Red crosses, experimental data, rectangular red boxes, uncertainty on the data; a), b) and c) mixture of glycerol and water (50/50 in volume), d) pure water.

E2. Straight line test

The pertinence of the value of the histogram bin size τ can be visualized by plotting the arrival time of the successive photons versus their numbers. The slope between two consecutive points is the delay between the detection of these two photons. This delay should follow a Poisson law with a constant mean. Consequently this graph should materialize a line with some Poissonian noise in the slope. If it is not the case it means that during the histogram step τ, the bead has explored different areas of the laser excitation volume with significant differences in intensities, assuming that the absorption cross-section and quantum yield are constant. A practical way of choosing τ is to decrease its value until the curve of the graph becomes a line.
Since the OPL signal is non linear with the laser irradiance, it is even more sensitive to a modification of the laser irradiance.

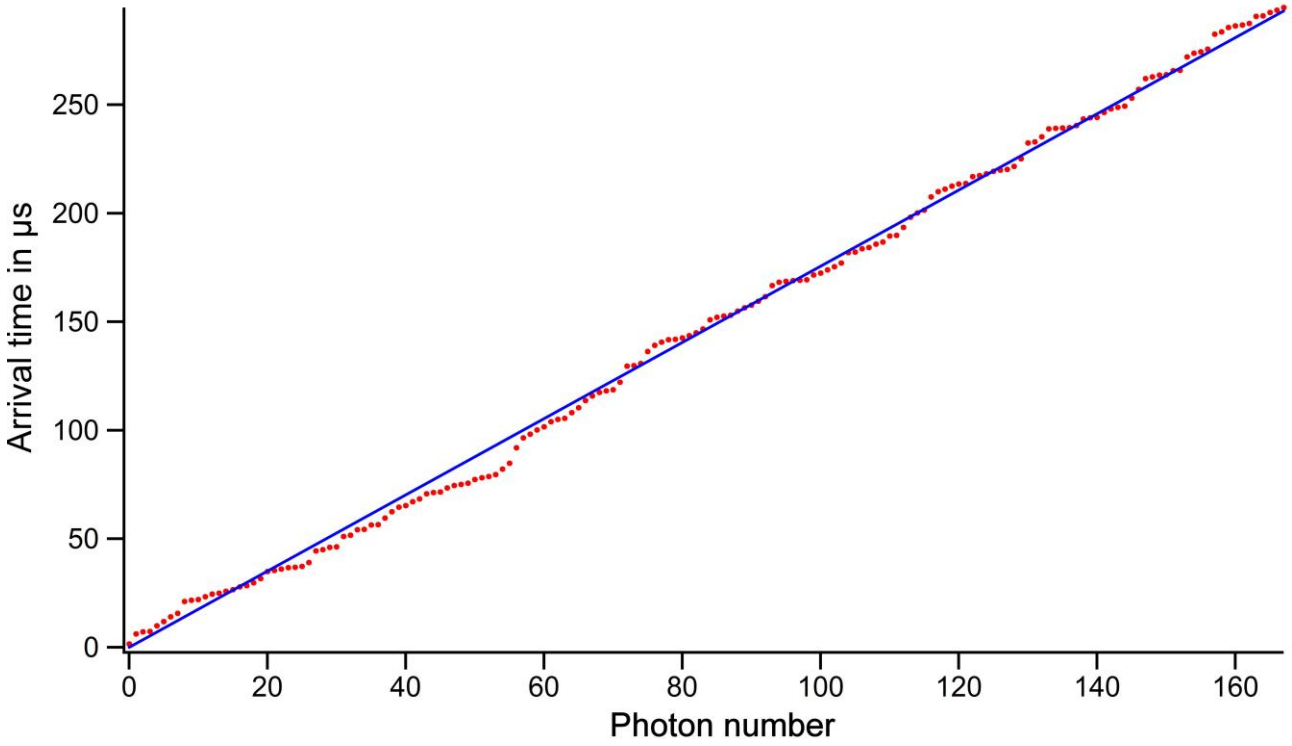

Figure S7. Repartition of the arrival times of OPL photons within a histogram with a bin size of 300µs. The fact that it can be described by a line validates the choice of 300µs for the histogram step τ

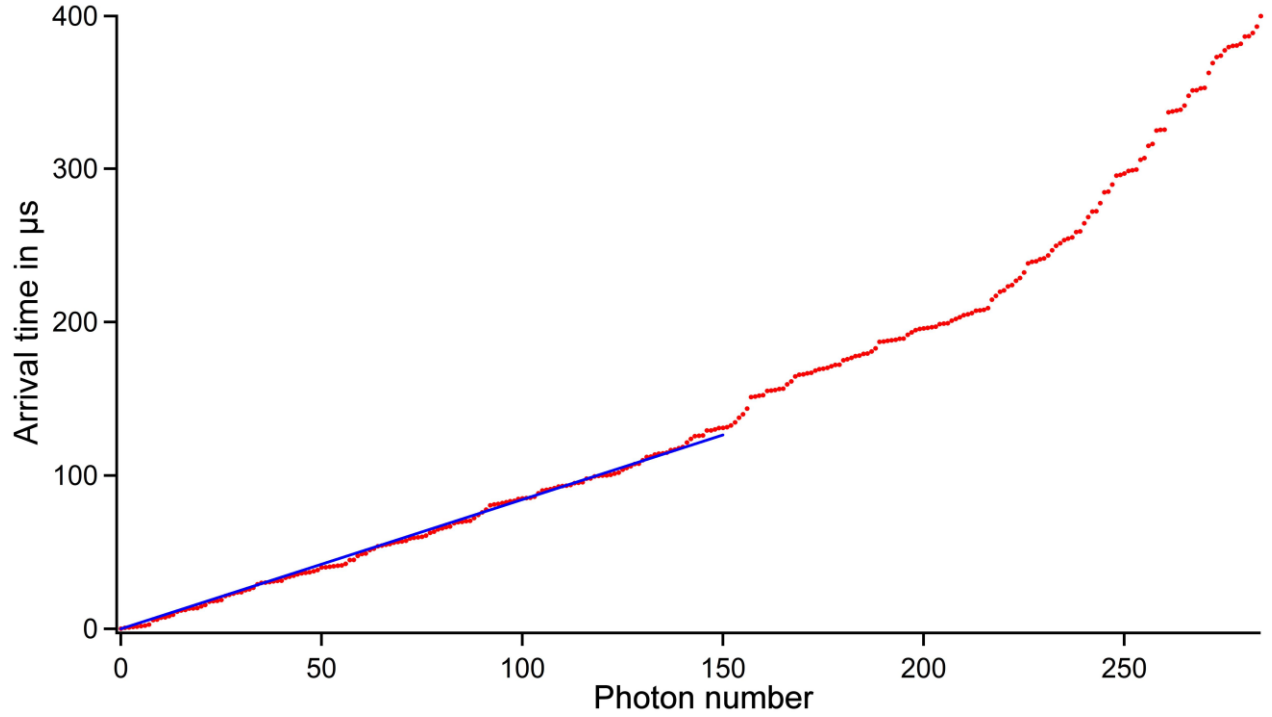

Figure S8. Repartition of the arrival times of OPL photons inside a histogram with a step of 400µs.

One can clearly observe several slopes in the curve that correspond to several explored areas of the laser excitation volume. It invalidates the choice of 400µs for the histogram step τ.

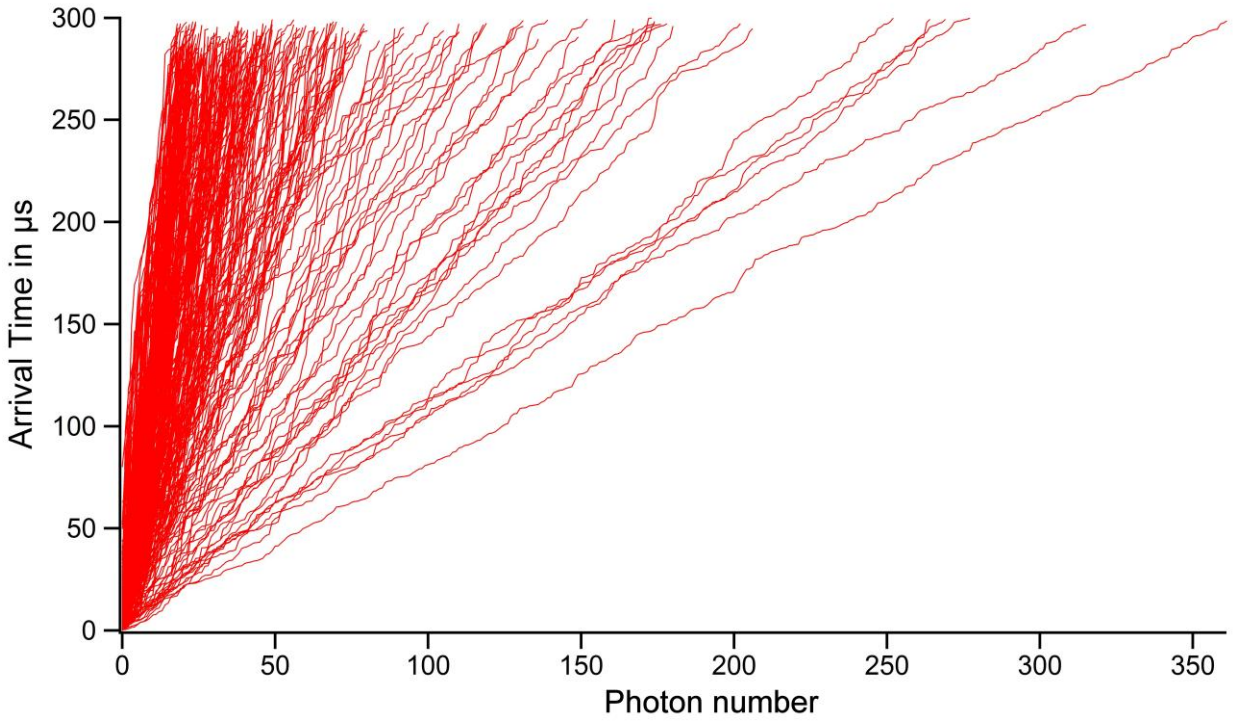

Figure S9. Plot of the line tests composing the saturation curve of a single bead in Fig.7 of the main text. Each line corresponds to one point of Fig.7. The step is 300µs.

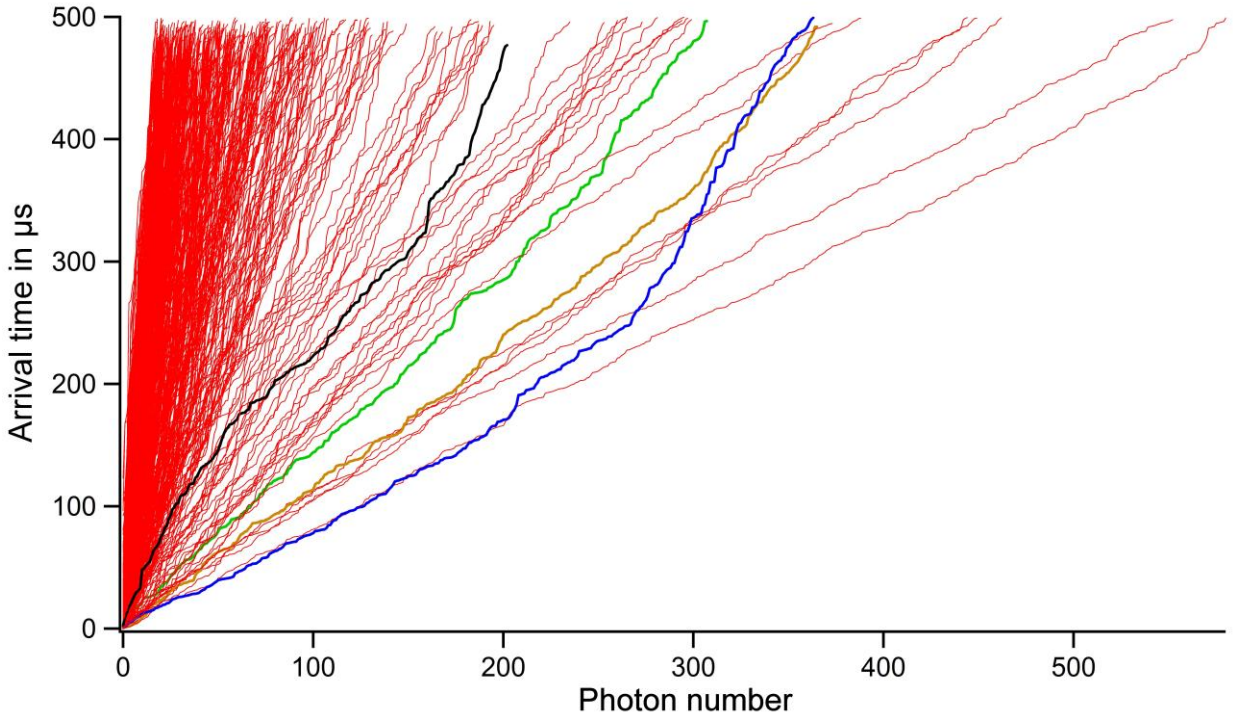

Figure S10. Plot of the line tests composing the saturation curve of a single bead if the step is equal to 500µs. Several traces exhibit a deviation to a straight line.

E3. Control experiment.

Probing this method requires particles large enough to efficiently scatter light. 100nm fluorescent latex beads are large enough to be detected by Rayleigh scattering but interestingly their fluorescence response does not have a easily readable trend with the laser power. This is possibly due to inter-quenching of the fluorescence inside the nanobead. Here, the experiment is controlled by plotting the Rayleigh scattering signals detected on the two lines of detection. 50 nm beads are diffusing in water. The time step is 50µs

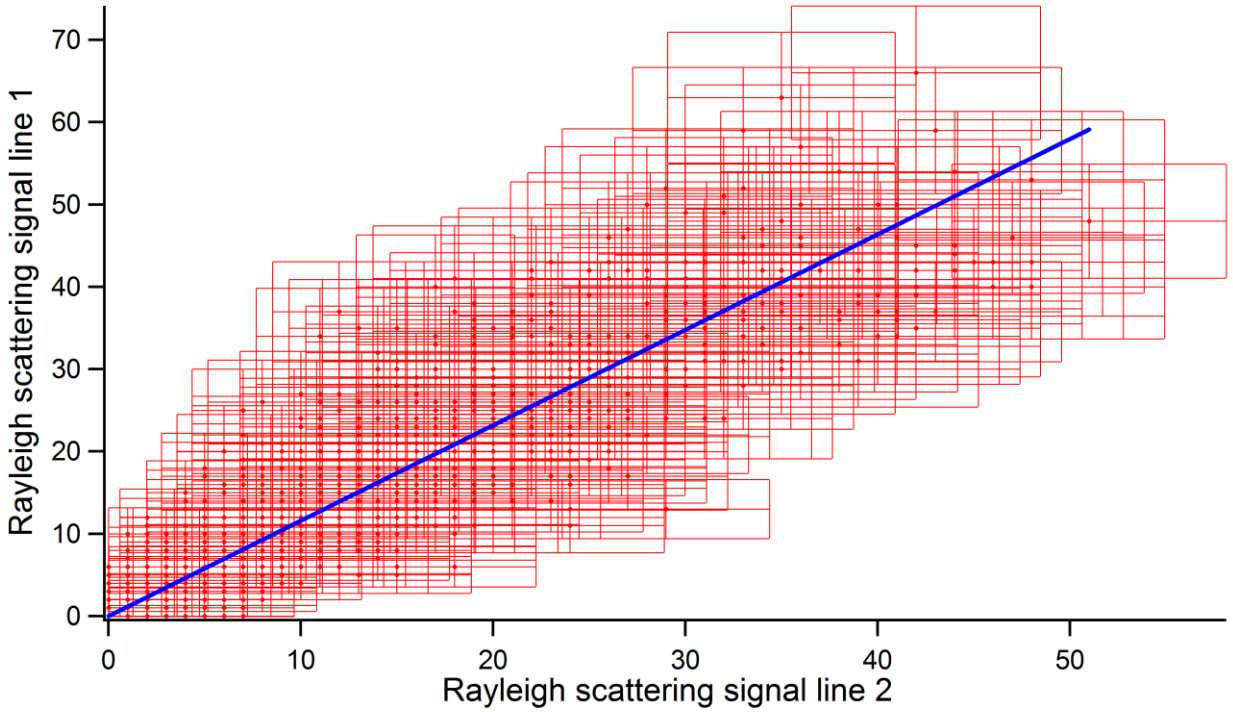

Figure S11. Control of the method.

F. Initial temperature of the gold particles.

The calculation of the temperature at the particle interface under pulsed excitation is generally described as a three-step process, namely the electronic excitation, the electron-phonon thermalization and the thermal equilibration at the interface with surrounding. The time dependence of the equilibration depends on the interface conductivity, which is of the order of 130 $MW/m^2.K$ for CTAB.[1] The heating of gold particles following the absorption of femtosecond pulses has been already described.[2,3] The characteristic time of electron-phonon thermalization is a few picosecondes.[4,5] Luminescence in the visible is a very fast process, with a characteristic time of the same order of pulse duration.[6] The thermalization process and the emission process overlap and the precise calculation of the temperature at the interface between the gold surface and the ligands is complex. The maximum initial value of the temperature derived from the eq. 26 of reference 3, assuming an infinite interface conductivity is 38°C for a particle of 50 nm diameter and an average irradiance of the pulsed excitation of $13kW/cm^2$ at 488 nm. The corresponding initial temperature for a continuous excitation of same irradiance is less than 3°C. This temperature is overestimated as explained above because of the different characteristic times of the processes. Moreover, the interface conductivity is finite, which contributes to lower the temperature at the interface. For an interface conductivity of about 130 $MW/m^2.K$, the value is roughly divided by a factor 3.[3]

1 A. J. Schmidt, J. D. Alper, M. Chiesa, G. Chen, S. K. Das and K. Hamad-Schifferli, *J. Phys. Chem. C*, 2008, **112**,13320.

2 O. Ekici, R. K. Harrisson, N. J. Durr, D. S. Eversole, M. Lee and A. Ben-Yakar, *J. Phys. D: Appl. Phys*., 2008, **41**, 185501.
3 G. Baffou and H. Rigneault, *Phys. Rev. B*, 2011, **84**,035415.
4 W. Huang, W. Qian, M. A. El-Sayed, Y. Ding, and Z. L. Wang, *J. Phys. Chem. C* , 2007, **111**, 10751.
5 J. H. Hodak, A. Henglein, and G. V. Hartland, *J. Chem. Phys.* 1999, **111**, 8613.
6 O. P. Varnavski, T. Goodson, M. B. Mohamed and M. A. El-Sayed, *Phys. Rev. B***,** 2005, **72**, 235405.
7 M. Loumaigne, A. Richard, J. Laverdant, D. Nutarelli and A. Débarre, *Nano Letters*, 2010, **10**, 2817.
8 M. Loumaigne, P. Vasanthakumar, A. Richard and A. Débarre, *Phys. Chem. Chem. Phys*., 2011, **13**, 11597.